Modeling Bessel Beam Surgery by Monte Carlo Simulation

Tarek Al-Saeed

Department Biomedical Engineering Departement, Faculty of Engineering, University of Helwan, Helwan(11517), Cairo, Egypt.

Corresponding author email: tarek1971@ieee.org

Received: Mar. 25, 2023, Revised: July 22, 2023, Accepted: July 26, 2023, Available Online: July 28, 2023 DOI: will be added soon

ABSTRACT— In this work we applied a Bessel beam (BB) to a layer of turbid medium. We applied the Monte Carlo simulation. This work emulates a tissue under surgery by a Bessel beam. Actually, the BB introduces less divergence. Thus it will be good for surgery. On the other part this is done by Monte Carlo simulation. Upon simulation we got family of curves to characterize absorption, reflection and scattering of this layer. Where we got numerical values of absorption, transmission and reflection of this layer. The curves are for layer thickness that varies along with varying scattering coefficient, absorption coefficient and anisotropy factor.

KEYWORDS: Bessel Beam, Monte Carlo Simulation, Surgery, Turbid Media.

I. INTRODUCTION

Durnin solved Helmholtz equation and find the zero order Bessel function as a solution. This solution has nondiffracting properties [1]. Bessel beam (BB) maintains collimation to a large distance propagation compared to the Gaussian beam [2]. The Bessel beam can be analyzed using digital holographic microscopy.

Bessel beam of zero order can be obtained by a narrow circular slit put in front of a convex lens at the focal plane of the lens. Another technique is by applying a collimated Gaussian beam to conic lens (axicon). Fabry-Perot can be used in generating Bessel beam and holography can also be used in Bessel beam generation [3-6].

Bessel beam has wide applications in medical research because of the ability of optical trapping and tweezing. Further, it can be used in super resolution microscopy. One application of Bessel beam is the in corneal surgery. Where the beam will be collimated along the cornea. More applications in optical coherence tomography [7,8]. Advanced optical tweezers for the study of cellular and molecular biomechanics [9]. Bessel beam can be used in imaging, optical communications etc.

The Bessel beam performs as a Bessel function of zero order in the transverse plane. Bessel beam has the advantage of non-diffracting so it propagates along a considerable distance without diffraction. It maintains its transversal profile and width along far distance and it does not spread out like ordinary beams i.e. Bessel beam has long depth of focus. Moreover, it has rotational symmetry, and the beam cross section is invariant along propagation direction. More practical applications in [10-14]. They considered transformation of Bessel beam intensity by passing the beam on a certain multilayer system [15]. In [16] they studied optical force exerted on Rayleigh particle by vector arbitrary order Bessel beam

The Bessel beam reconstructs itself after partial passage of an obstacle or obstruction, where parts of the beam re-interfere to obtain the original structure of the transverse field. Bessel beam is the interference of two Hankel beams going in opposite directions. We have Hankel function of the first and second kind. This

reconstruction is called self-healing. The BB repairs itself.

In [17] they considered BB spatially truncated. Presented a study of the spiral beam base on a truncated Bessel beam and plane wave. The spiral beam maintains its shape along propagation

Bessel beam is the interference of two Hankel beams going in opposite directions. We have Hankel function of the first and second kind. This reconstruction is called self-healing.

In this work we model the BB surgery as a single turbid layer where we apply a BB to this layer which cuts in this layer. We analyze the problem by Monte Carlo simulation [18]. We got absorption, reflection and transmission and we discuss the effect of varying layer thickness (LT).

This paper is organized as follows. Section 2 presents theoretical analysis. Section 3 presents the obtained numerical results. Section 4 presents discussion and Section 5 presents conclusion.

II. THEORETICAL ANALYSIS

Bessel beam can be generated by many different ways. In this work we consider a beam generated putting a circular slit (annulus) in front of a lens.

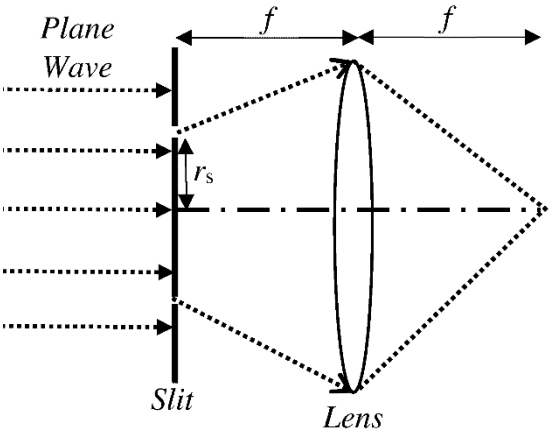

Fig. 1. Schematic of generation of Bessel beam. Incident plane wave is confronted by a circular slit and focused at distance f.

The field of the slit is given by

$$E_{slit} = A\delta\left(r - r_s\right). \tag{1}$$

The field beyond the lens is proportional to the Fourier transform which is given by

$$E_{beyond}(x,y) = \frac{1}{j\lambda f}\int_{-\infty}^{+\infty}\int_{-\infty}^{+\infty} dx'dy' E_{slit}\left(x',y'\right)\times \times \exp\left[\frac{j2\pi\left(xx'+yy'\right)}{\lambda f}\right], \tag{2}$$

$$E_{beyond}(r) = \frac{1}{j\lambda f}\int_{0}^{\infty}\int_{0}^{2\pi} \rho d\rho d\phi E_{slit}(\rho,\phi)\times \times \exp\left[\frac{j2\pi r\rho\left(\cos\phi\cos\theta+\sin\phi\sin\theta\right)}{\lambda f}\right], \tag{3}$$

$$E_{beyond}(r) = \frac{1}{j\lambda f}\int_{0}^{\infty}\int_{0}^{2\pi} \rho d\rho d\phi E_{slit}(\rho)\times \times \exp\left[\frac{j2\pi r\rho\left(\cos\phi\cos\theta+\sin\phi\sin\theta\right)}{\lambda f}\right]. \tag{4}$$

Due to symmetry in azimuthal direction, we have

$$E(r) = \frac{1}{\lambda f}\int_{0}^{\infty}\int_{0}^{2\pi} \rho d\rho d\phi E_{slit}(\rho)\times \times \exp\left[\frac{j2\pi r\rho\cos(\phi-\theta)}{\lambda f}\right], \tag{5}$$

$$E_{beyond}(r) = \frac{2\pi}{j\lambda f}\int_{0}^{\infty} d\rho\rho E_{slit}(\rho) J_0\left(\frac{2\pi\rho}{\lambda f}r\right), \tag{6}$$

$$E_{beyond}(r) = A\frac{2\pi r_s}{j\lambda f} J_0\left(\frac{2\pi r_s}{\lambda f}r\right). \tag{7}$$

The intensity is given by

$$I(r) = \left(J_0(k_0 r\sin\beta)\right)^2 = \left(J_0(k_r r)\right)^2, \tag{8}$$

where,

$$\sin\beta = \frac{r_s}{f}, \tag{9}$$

$$k_r = k_0\sin\beta. \tag{10}$$

The probability density function (pdf) of the radius of the Bessel beam is derived as the incremental power contained in a circular strip of length *dr*:

$$2\pi I(r)\,r dr, \tag{11}$$

$$u = k_r r. \tag{12}$$

We introduce function $G(u)$ given by

$$G(u) = 1 \qquad 0 \le u \le u_{\max}, \tag{13}$$

where G is a normalized test function.

Actually, u_{max} is given as a truncation of the Bessel function for twelve side lobes. The pdf of this function is given by

$$\text{pdf}\,(u) = Eu, , \tag{14}$$

where E is a constant given by:

$$E = \frac{1}{\int_0^{u_{\max}} u du} = \frac{2}{u_{\max}^2}. \tag{15}$$

Thus the probability density function is given by:

$$\text{pdf} = \frac{2u}{u_{\max}^2}. \tag{16}$$

The cumulative density function (cdf) is given by:

$$\begin{aligned} &\text{cdf}\,(u) = \int_0^u pdf\,(u) du, \\ &\int_0^u \frac{2u}{u_{\max}^2} du = \frac{u^2}{u_{\max}^2}. \end{aligned} \tag{17}$$

We sample this cdf by using random variable, U(x:1), from zero to one given as:

$$\xi = U(0:1). \tag{18}$$

Then we invert this cdf as:

$$u = u_{\max}\sqrt{\xi}, \tag{19}$$

$$\text{icdf}\,(\xi) = u_{\max}\sqrt{\xi} \tag{20}$$

Procedure for photon launching (accept/rejection technique) is given in appendix.

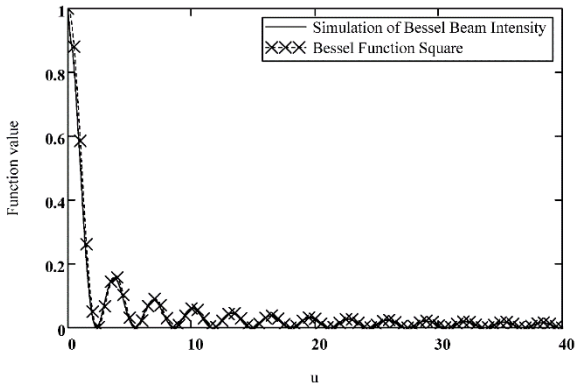

Fig. 2. Verification of Bessel beam. The line curve gives the simulation intensity upon using the appendix accept/rejection technique. The dotted-crosses curve gives the Bessel square as a function of u.

In Fig. 2, we verify our accept/rejection technique to simulate the BB intensity where we compare it with the square of the Bessel function of zero order. It gives excellent results.

Finally, we use this launching technique to find the absorption, reflection, and transmission of a layer of tissue (turbid medium) obtaining by Monte Carlo simulation (MCS) [18]. MCS need four parameters. First refractive index. Second absorption coefficient which accounts for absorption. Third is scattering coefficient which accounts for scattering. Fourth anisotropy factor which is the average of cosine of the polar scattering angle. Finally, the polar scattering angle is governed by the Henyey-Greenstein function [18].

III. NUMERICAL RESULTS

We applied MCS to a tissue and got absorption, reflection, and transmission. We vary the parameters of the structure like LT, anisotropy factor, *g*, scattering coefficient, absorption coefficient and wavelength. Further, we assume matched refractive index. The problem under

investigation is plotted in Fig. 3. Moreover, we used 5×105 photon packets in each simulation. To sample the problem, we have $\Delta x=\Delta y=\Delta z=20\mu m$. In our work, the Bessel function is infinite, but we truncate the Bessel function to twelve side lobes. This is a good approximation.

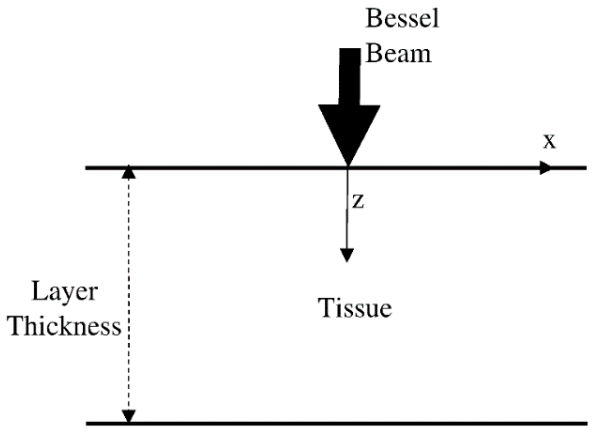

Fig. 3. Schematic of the problem under investigation

In the following we will present the results of each parameter in a separate subsection.

A. Profile of absorption, reflection, and transmission

In Fig. 4, we have plotted the profile of the absorption, reflection, and transmission. The simulation parameters are: b=30º, l=2mm, LT=400mm, absorption coefficient ma=0.2cm^{-1}, scattering coefficient ms=100cm^{-1}, and anisotropy factor g=0.9. For Fig. 4(a), we have plotted the absorption profile at y=0, z=4Dz and as a function of x. Figure 4(b) profile of reflection. It shows symmetric sharp spike. In Fig. 5(c), it shows symmetric spike of transmission. All profiles give sharp peaks with symmetric character around the axis of the BB.

For Figs. 4(b) and 4(c) we have the profile at y=0 and as a function of x.

B. Total absorption, reflection and transmission vs. LT for different anisotropy factor

In this subsection we vary the LT and obtain the total absorption, total reflection and total transmission. We calculate this for different anisotropy factor g=0.90, 0.95, and 0.99. The other simulation parameters are: β=30º, λ=1.3μm, μa=0.1cm^{-1}, μs=100cm^{-1}.

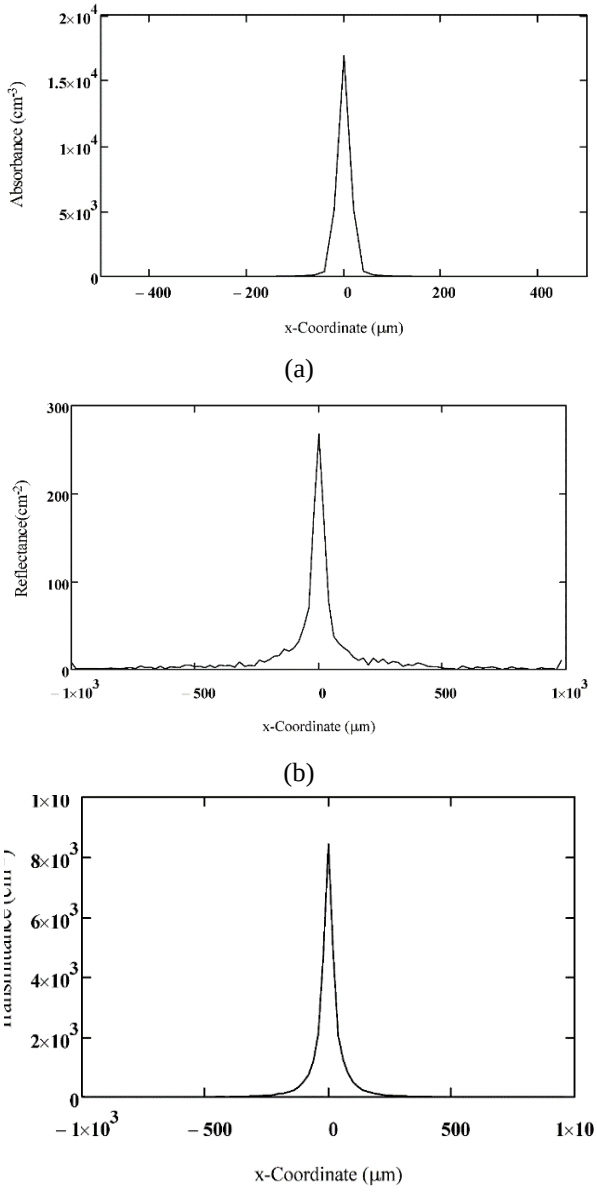

Fig. 4. (a) absorption profile along x direction, (b) reflection profile for y=0 and as a function of x, (c) transmission profile for y=0 and as a function of x. The simulation parameters are: β=30º, λ=2μm, LT=400μm, absorption coefficient μa=0.2cm^{-1}, scattering coefficient μs=100cm^{-1}, anisotropy factor g=0.9

In Fig. 5, we have plotted total absorption, reflection, and transmission vs. layer thickness for different g. Absorption increases with increase in LT. Further, as g increases absorption decreases. Reflection increases as LT increases and as g increases absorption decreases. Transmission decreases, as LT

increases and as g increases, transmission increases.

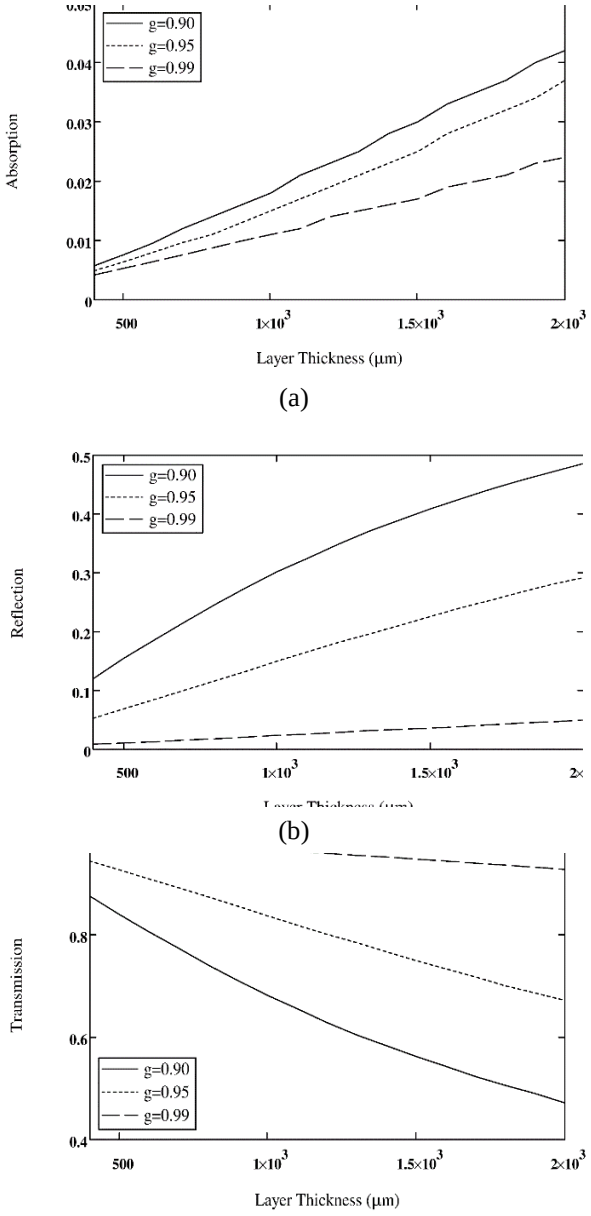

Fig. 5. (a) Total absorption, (b) reflection and (c) transmission as a function of LT for different g. We calculate this for different anisotropy factor g=0.90, 0.95 and 0.99. The other simulation parameters are: β=30º, λ=1.3μm, μa=0.1cm^{-1}, and μs=100cm^{-1}.

C. Total absorption, reflection and transmission vs. LT for different μs.

In this subsection we vary the LT and obtain the total absorption, total reflection and total transmission. We calculate this for different μs=75, 100, and 125 cm^{-1}. The other simulation parameters are: β=30º, λ=1.3μm, μa=0.1cm^{-1}, and g=0.9.

In Fig. 6, we have plotted parameters as a function of LT for different μs. Absorption increases as layer thickness increases. Further, as μs increases absorption increases. As LT increases reflection increases and as μs increases reflection increases. Further, as LT increases, transmission decreases and as μs increases, transmission decreases.

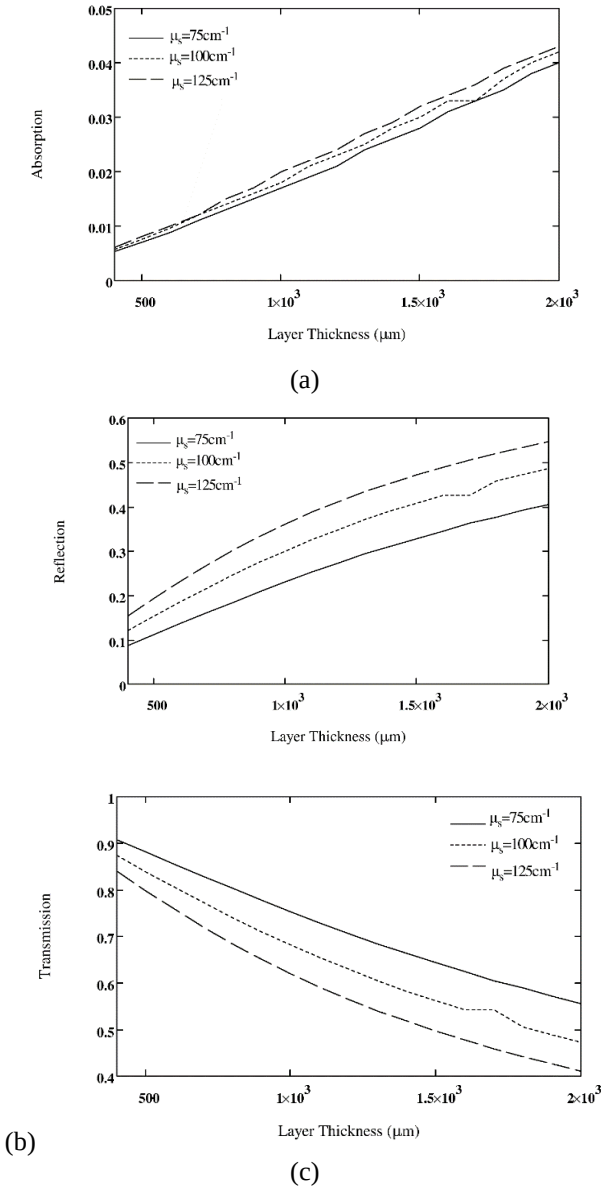

Fig. 6. (a) Total absorption, (b) reflection and (c) transmission vs layer thickness and for different μs of 75, 100, and 125 cm^{-1}. The other simulation parameters are: β=30º, λ=1.3μm, μa=0.1cm^{-1}, and g=0.9.

D. Total absorption, reflection and transmission vs. LT for different μa.

In this subsection we vary the LT and obtain the total absorption, total reflection and total transmission. We calculate this for different μa=0.2, 0.4, and 0.6 cm^{-1}. The other simulation parameters are: β=30º, λ=1.3μm, μs=100cm^{-1}, and g=0.9.

In Fig. 7, we have plotted parameters as a function of LT for different μa.

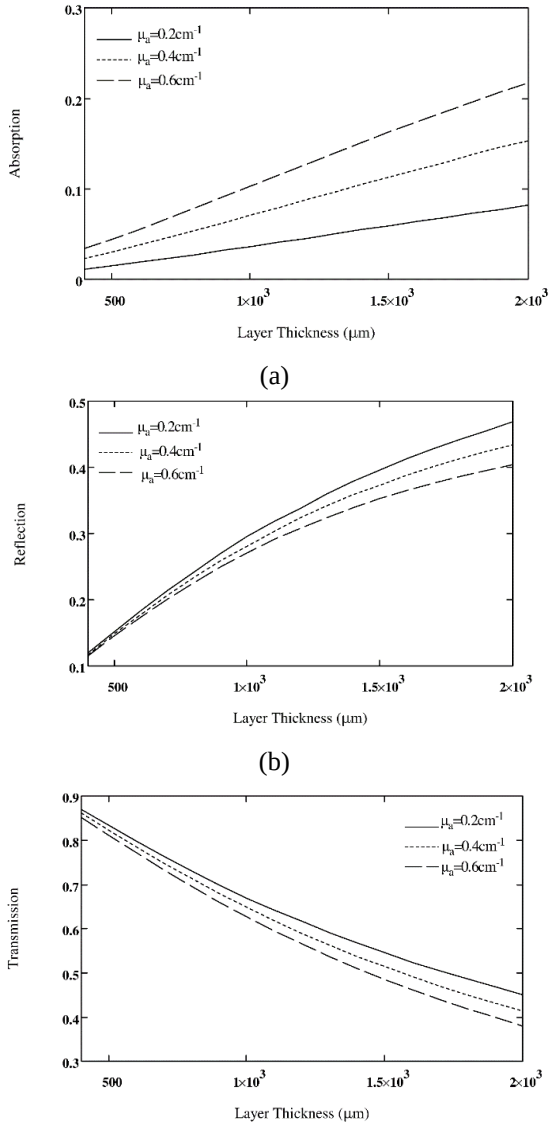

Fig. 7. (a) Total absorption, (b) total reflection and (c) total transmission vs layer thickness and for different μa. We calculate this for different μa=0.2, 0.4, and 0.6 cm^{-1}. The other simulation parameters are: β=30º, λ=1.3μm, μs=100cm^{-1}, and g=0.9.

Absorption increases as LT increases and as μa increases absorption increases. As LT increases reflection increases and as μa increases reflection decreases. Further, transmission decreases, as LT increases and it decreases, as absorption coefficient increases.

E. Spectra of Total absorption, reflection and transmission for different LT

In this subsection we vary the wavelength and obtain the total absorption, total reflection and total transmission. The other simulation parameters are: β=30º, μa=0.1cm^{-1}, μs=100cm^{-1}, and g=0.9.

In Fig. 8, absorption shows constant dependence on wavelength. Further, total reflection and total transmission shows also constant wavelength dependence.

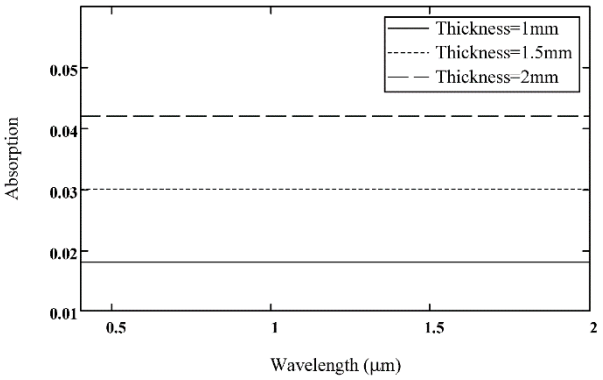

Fig. 8. Total absorption spectra for different layer thickness. which shows constant response. The same is for reflection and transmission. The other simulation parameters are: β=30º, λ=1.3μm, μa=0.1cm^{-1}, μs=100cm^{-1}, and g=0.9.

F. Peaks of absorption

We calculate absorption and find the peaks of absorption along the z-axis. The simulation parameters are: β=30º, λ=2μm, μa=0.2, 0.4, and 0.6cm^{-1}, μs=100cm^{-1}, and g=0.9, layer thickness=400μm. In Fig. 9, we have plotted the value of the peak at the axis. The peak decreases as depth increases and increases as μa increases.

G. Full width at half maximum for absorption profile

In this subsection we calculate the full width at half maximum (FWHM) for absorption profile

along x-axis for different depth positions where y=0. The simulation parameters are: β=30º, λ=2μm, μa=0.2, 0.4, and 0.6cm^{-1}, μs=100cm^{-1}, and g=0.9, layer thickness=400μm. In Fig. 9, peaks of profile of absorption vs. depth is presented, where peaks decrease as a function of depth.

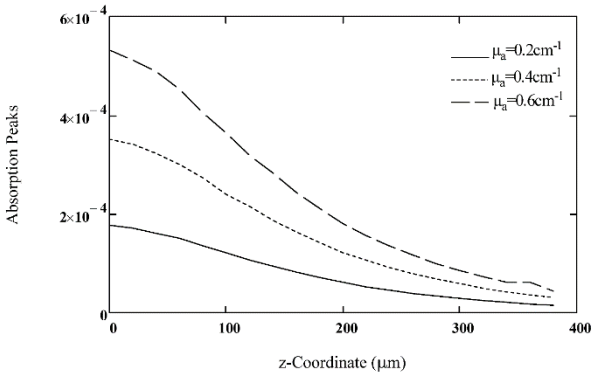

Fig. 9. Absorption peaks along the z-axis. They decrease along the z-coordinate. The simulation parameters are: β=30º, λ=2μm, μa=0.2, 0.4, and 0.6cm^{-1}, μs=100cm^{-1}, g=0.9, and LT=400μm

In Fig. 10, we have plotted the FWHM of the absorption profile along the depth where FWHM increases as depth increases and show no appreciable variation as μa increases. The curves for different μa overlap.

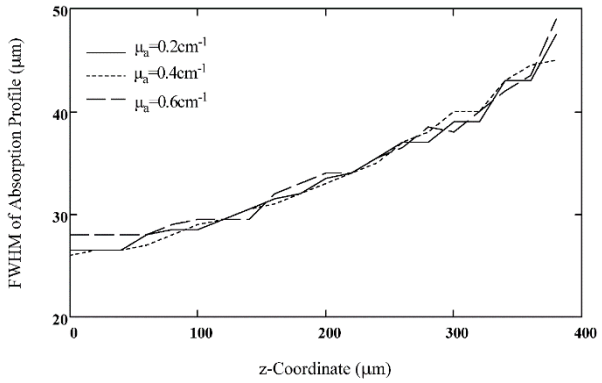

Fig. 10. FWHM for absorption profile along x-direction as a function of depth for different values of μa. The curves show same response of monotonic increasing performance

IV. DISCUSSION

We truncate the zero order BB to some extent. Of twelve lobes. Then in Fig. 2, we verify our accept/rejection technique where simulation of the BB intensity with this technique come in same performance to the square of the Bessel function. In Fig. 4, we have plotted the profile of absorption, reflection and transmission.

We have a fact that as LT increases total absorption increases. Further, total reflection increase as LT increases and transmission decreases as LT increases. This applies for Figs. 5, 6, and 7. Actually, absorption will increase as LT increases because there is more chance of absorbing the photon packet. Transmission will decrease as LT increases because the photon packet has no chance to escape the medium as it will be absorbed. Finally, reflection will increase because the photon packet will have a chance to emerge backwardly.

Moreover, as g increases absorption decreases, reflection decreases and transmission increases. Absorption will decrease as g increases because the photon packet will be scattered more forwardly and emerge more from the layer in the form of transmission which will increase by g. Reflection decreases as g increases because the photon packet will scatter more in forward direction.

As ms increases, absorption increases, reflection increases, and transmission decreases. Because as μs increases photon packet will scatter more so transmission will be less and it will have a chance for backward emerging so reflection increases. Moreover, as μs increases absorption increases because of more extinction chances in the layer.

Finally, as μa increases, absorption increases, reflection decreases, and transmission decreases. This is because as μa absorption increases naturally and the photon packet will have more extinction events in the layer before it emerge backwardly. From the same concept transmission will decreases.

In Fig. 8, spectra of absorption, reflection, and transmission show no variations. In Fig. 9, we have plotted the value of the absorption peak. The peak decreases, as depth increases, and increases, as μa increases. It is natural because as μa increases axial absorption increases. In Fig. 10, we have plotted the FWHM of the absorption profile along the depth where

FWHM increases as depth increases and show no appreciable variation as μa increases. The absorption profile widens as depth (z-axis) increases.

It should be noted that the use of Gaussian beam In treatment it will suffer from high divergence. The collimated range is governed to small distance known Rayleigh distance which is small compared to the Bessel beam [19].

V. CONCLUSION

In this paper we succeeded to model the Bessel beam (BB) by an accept\rejection technique. We got results of absorption, reflection and transmission for varying the parameters of the tissue. We found that as layer thickness (LT) increases, total absorption increases, total reflection increases, and total transmission decreases.

Moreover, as anisotropy factor, *g*, increases total absorption decreases, total reflection decreases, and total transmission increases. As scattering coefficient, μs, increases, total absorption increases, so the photon will remain in the tissue more.

Also, as absorption coefficient , μa, increases, reflection increases, transmission decreases, and absorption increases. Spectra of absorption, reflection, and transmission show no variations. The absorption peak decreases, as depth increases, and increases as μa increases. The absorption profile widens as depth (z-axis) increases.

APPENDIX

Procedure for photon launching (accept/rejection technique):

Get a random number $\xi_1 = U(0:1)$.

$Y = \text{icdf}\left(\xi_1\right)$,

$$\text{Ratio} = \frac{J_0^2(u)}{G(u)}$$

Get a random number $\xi_2 = U(0:1)$

If $\text{Ratio} \geq \xi_2$ return Y and break

Go to step (1)

Upon obtaining Y from the above procedure we get another random number ξ_3=U(0:1) and we get the x y coordinates as

$$x = \frac{Y}{k_r}\cos\left(2\pi\xi_3\right); \qquad y = \frac{Y}{k_r}\sin\left(2\pi\xi\right) \tag{A1}$$

REFERENCES

[1] J. Durnin "Exact Solutions for Nondiffracting Beams. I. The Scalar Theory," J. Opt. Soc. Am. A, Vol. 4, pp. 651–654, 1987.

[2] J. Durnin, J. Miceli, and J.H. Eberly, "Comparison of Bessel and Gaussian beams," Opt. Lett., Vol. 3, pp.79–80, 1988.

[3] M. Duocastella and C. B. Arnold, "Bessel and annular beams for materials processing," Laser Photon. Rev., Vol. 6, pp. 607-621, 2012.

[4] B.E.A. Saleh and M.C. Teich, *Fundamentals of Photonics*, Wiley-Interscience, pp. 120-126, New York,1991.

[5] J.W. Goodman, *Introduction to Fourier optics*, *Roberts, Englewood, Colorado*, 2005.

[6] T. Čižmár, V. Kollárová, X. Tsampoula, F. Gunn-Moore, W. Sibbett, Z. Bouchal, and K. Dholakia, "Generation of multiple Bessel beams for a bio- photonics workstation," Opt. Exp., Vol. 16, pp. 14024–35, 2008.

[7] Z. Ding, H. Ren, Y. Zhao, J.S. Nelson, and Z. Chen, "High-Resolution Optical Coherence Tomography Over a Large Depth Range with an Axicon Lens," Opt. Lett., Vol. 27, pp. 243–245, 2002.

[8] H. Martin, P. Kumar, A. Henning, and X. Jiang, "Extended sub-surface imaging in industrial OCT using 'non-diffracting' Bessel beams," CIRP Annals - Manufacturing Technology Vol. 69, pp. 493-496, 2020.

[9] B. GJ, S. HT, and H. AJ, "Advanced optical tweezers for the study of cellular and molecular biomechanics," IEEE Biomed Eng., Vol. 50, pp. 121-125, 2003.

[10] L. Han, Y.P. Han, Z.W. Cui, and J.J. Wang, "Expansion of a zero-order Bessel beam in spheroidal coordinates by generalized Lorenz–Mie theory," J. Quant. Spectrosc. Radiat. Transf., Vol. 147, pp. 279-287, 2014.

[11] G. DG., "A revolution in optical manipulation," Nature, Vol. 424, pp. 810-816, 2003.

[12] T. Wulle and S. Herminghaus, "Nonlinear optics of Bessel beams," Phys. Rev. Lett. 70:1401, 1993.

[13] B. Hafizi, E. Esarey, and P. Sprangle,"Laser-driven acceleration with Bessel beams," Phys. Rev. E, Vol. 55, pp. 3539-3545, 1997.

[14] H. Little, C. Brown, V. Garcés-Chávez, W. Sibbett , and K. Dholakia, "Optical guiding of microscopic particles in femto second and continuous wave Bessel light beams," Opt Exp. Vol. 12, pp. 2560-2565, 2004.

[15] A.V. Novitsky, "Intensity transformation of vector Bessel beams using a multilayer system," Opt. Commun., Vol. 281, pp. 5310–5314 , 2008.

[16] R.Yang and R. Li, "Optical force exerted on a Rayleigh particle by a vector arbitrary-order Bessel beam," J. Quant. Spectrosc. Radiat. Transf., Vol. 178, pp. 230–243, 2017.

[17] M. Anguiano-Morales, D.P. Salas-Peimbert, G. Trujillo-Schiaffino, D. Monzon-Hernández, and N. Toto-Arellano, "Bessel beam spatially truncated," Opt. Commun., Vol. 284, pp. 1504–1509, 2011.

[18] L. Wang, S.L. Jacques, and L. Zheng, "MCML-Monte Carlo modeling of light transport in multi-layered tissues," Comput. Methods Programs Biomed., Vol. 47, pp. 131–146, 1995.

[19] K. Zhang and D. Li, *Electromagnetic Theory for microwaves and optoelectronics*, Springer-Verlag Berlin, Heidelberg, 2nd Ed., 2008.

Tarek Al-Saeed got B.Sc. and M.Sc. in electronics and communications engineering from Faculty of Engineering in Ain-Shams University in 1994 and 1999, respectively. He got Ph.D. in biomedical engineering from Faculty of Engineering of Helwan University in 2006. He got another Ph.D. in electronics and communications engineering from Faculty of Engineering in Ain-shams University in 2013. Dr Tarek Al-Saeed research interests are biomedical optics and the subjects of interest are FTIR, OCT and Monte Carlo.

THIS PAGE IS INTENTIONALLY LEFT BLANK.